Sādhanā, Vol. 9, Part 4, December 1986, pp. 255–269. © Printed in India.

Noise reduction with perforated three-duct muffler components

K NARAYANA RAO* and M L MUNJAL†

Department of Mechanical Engineering, Indian Institute of Science, Bangalore 560 012, India

*Present address: Mechanical Engineering Department, University College of Engineering, Osmania University, Hyderabad 500 007, India

†Present address: Department of Mechanical Engineering, University of Calgary, 2500 University Drive NW, Calgary, Alberta, Canada T2N 1N4

MS received 21 March 1986; revised 28 May 1986

Abstract. This paper describes the authors' distributed parameter approach for derivation of closed-form expressions for the four-pole parameters of the perforated three-duct muffler components. In this method, three simultaneous second-order partial differential equations are first reduced to a set of six first-order ordinary differential equations. These equations are then uncoupled by means of a modal matrix. The resulting 6×6 matrix is reduced to the 2×2 transfer matrix using the relevant boundary conditions. This is combined with transfer matrices of other elements (upstream and downstream of this perforated element) to predict muffler performance like noise reduction, which is also measured. The correlation between experimental and theoretical values of noise reduction is shown to be satisfactory.

Keywords. Mufflers; noise control; transfer matrix method.

1. Introduction

The majority of the commercial mufflers used on internal combustion engines contain one or more perforated tubes. These may interact with the surrounding annular cavity as in a Helmholtz resonator, or may conduct the gases as in plug mufflers and three-duct cross-flow or reverse-flow mufflers. Unfortunately, however, analysis of such perforated-element mufflers was not known until a few years ago, with the result that the design of commercial mufflers was based on trial and error.

Recently, the authors developed and presented a generalized decoupling method for the analysis of perforated-element mufflers with and without mean flow, wherein the mean flow Mach numbers are allowed to have their actual (unequal) values (Rao & Munjal 1984). But the method was demonstrated for two-duct elements only. This method makes use of the distributed parameter approach in

contrast to Sullivan's segmentation approach (Sullivan 1979a, b), where a perforated element is notionally divided into a number of segments.

The present work extends the distributed parameter approach to three-duct muffler element configurations by removing the ambiguities in evaluation of the eigenvalues of the characteristic matrix. The three coupled partial differential equations for wave propagation have been solved using the authors' generalized decoupling approach with and without mean flow incorporating the relevant exact boundary conditions. Explicit expressions have been derived for four-pole parameters of the cross-flow expansion chamber as well as the reverse-flow expansion chamber, shown in figure 1. The transfer matrices so derived have been checked experimentally by comparing the predicted values of noise reduction with those observed experimentally.

2. The coupled governing equations

Implicit in the following equations, and the solution thereof, are certain assumptions that are typical of automotive muffler analysis, viz,

(i) working in the frequency domain, all acoustic variables are made to have harmonic time-dependence everywhere;
(ii) at the frequencies of interest, only plane waves would propagate; higher order modes could be ignored;
(iii) mean flow velocities are small enough; the flow is incompressible;
(iv) heat transfer and viscosity effects are neglected; all processes are isentropic;

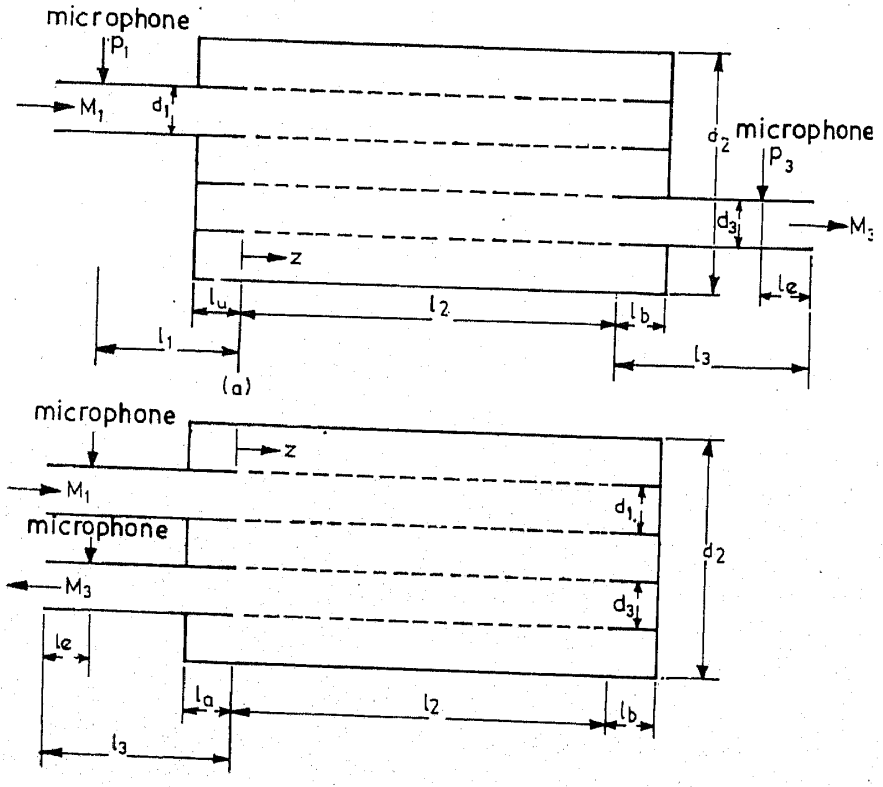

Figure 1. Three-duct muffler configurations: **a.** cross-flow expansion chamber, **b.** reverse-flow expansion chamber.

(v) mean flow gradients along and across the duct are neglected. The same holds for mean pressure and mean density;

(vi) velocity of cross flow is assumed to be uniform all over the perforate. This allows us to assume a uniform acoustic impedance for the perforate.

For the three-duct model as shown in figure 2, the mass continuity equations may be written as (Sullivan & Crocker 1978)

$$\rho_0 \frac{\partial w_1}{\partial z} + W_{o_1} \frac{\partial \rho_1}{\partial z} + \frac{4}{d_1} \rho_0 u_{1,2} = -\frac{\partial \rho_1}{\partial t}, \tag{1}$$

for duct 1 of diameter d_1,

$$\rho_0 \frac{\partial w_2}{\partial z} + W_{o_2} \frac{\partial \rho_2}{\partial z} - \frac{4d_1}{(d_2^2 - d_1^2 - d_3^2)} \rho_0 u_{1,2} + \frac{4d_3}{(d_2^2 - d_1^2 - d_3^2)} \rho_0 u_{2,3} = -\frac{\partial \rho_2}{\partial t}, \tag{2}$$

for duct 2 of diameter d_2, and

$$\rho_0 \frac{\partial w_3}{\partial z} + W_{o_3} \frac{\partial \rho_3}{\partial z} - \frac{4}{d_3} \rho_0 u_{2,3} = -\frac{\partial \rho_3}{\partial t}, \tag{3}$$

for duct 3 of diameter d_3. The notation is given in appendix D.

The corresponding momentum equations are

$$\rho_0 \left(\frac{\partial w_j}{\partial t} + W_{o_j} \frac{\partial w_j}{\partial z} \right) = -\frac{\partial p_j}{\partial z}, \quad j = 1, 2, 3. \tag{4), (5), (6}$$

The radial momentum at interfaces of duct 1 and duct 3 result in the equations

$$u_{1,2}(z, t) = [p_1(z, t) - p_2(z, t)]/(\rho_0 c_0 \zeta_1), \tag{7a}$$

and

$$u_{2,3}(z, t) = [p_2(z, t) - p_3(z, t)]/(\rho_0 c_0 \zeta_2), \tag{7b}$$

respectively.

Assuming that the fluid is an ideal gas and the process involving wave propagation is isentropic,

$$p_j = \rho_j c_0^2, \quad j = 1, 2, 3. \tag{8}$$

For harmonic time dependence,

$$p_j(z, t) = p_j(z)\, e^{i\omega t}, \quad j = 1, 2, 3, \tag{9a}$$

and

$$u_{j,k}(z, t) = u_{j,k}(z)\, e^{i\omega t}, \quad j = 1, 2, \quad k = 2, 3. \tag{9b}$$

Substituting (7a), (7b), (8), (9a) and (9b) into (1) to (6) and eliminating ρ_1, ρ_2, ρ_3, $u_{1,2}$, $u_{2,3}$, w_1, w_2 and w_3, yields the following three coupled differential equations for ducts 1, 2 and 3, respectively (Munjal 1986),

$$\left[\frac{d^2}{dz^2}-\frac{iM_1}{1-M_1^2}\left(\frac{k_a^2+k^2}{k}\right)\frac{d}{dz}+\frac{k_a^2}{1-M_1^2}\right]p_1(z)$$

$$+\left[\frac{iM_1}{1-M_1^2}\left(\frac{k_a^2-k^2}{k}\right)\frac{d}{dz}-\frac{k_a^2-k^2}{1-M_1^2}\right]p_2(z)=0, \tag{10}$$

$$\left[\frac{iM_2}{1-M_2}\left(\frac{k_b^2-k^2}{k}\right)\frac{d}{dz}-\frac{k_b^2-k^2}{1-M_2^2}\right]p_1(z)$$

$$+\left[\frac{d^2}{dz^2}-\frac{iM_2}{1-M_2^2}\frac{(k_b^2+k_c^2)}{k}\frac{d}{dz}+\frac{k_b^2+k_c^2-k^2}{1-M_2^2}\right]p_2(z)$$

$$+\left[\frac{iM_2}{1-M_2^2}\left(\frac{k_c^2-k^2}{k}\right)\frac{d}{dz}-\frac{k_c^2-k^2}{1-M_2^2}\right]p_3(z)=0, \tag{11}$$

$$\left[\frac{iM_3}{1-M_3^2}\left(\frac{k_d^2-k^2}{k}\right)\frac{d}{dz}-\frac{k_d^2-k^2}{1-M_3^2}\right]p_2(z)$$

$$+\left[\frac{d^2}{dz^2}-\frac{iM_3}{1-M_3^2}\left(\frac{k_d^2+k^2}{k}\right)\frac{d}{dz}+\frac{k_d^2}{1-M_3^2}\right]p_3(z)=0, \tag{12}$$

where

$$k=\frac{\omega}{c_0},\quad M_1=\frac{W_{o_1}}{c_0},\quad M_2=\frac{W_{o_2}}{c_0},\quad M_3=\frac{W_{o_3}}{c_0},$$

$$k_a^2=k^2-\frac{i4k}{d_1\zeta_1},\quad k_b^2=k^2-\frac{i4kd_1}{(d_2^2-d_1^2-d_3^2)\zeta_1},$$

$$k_c^2=k^2-\frac{i4kd_3}{(d_2^2-d_1^2-d_3^2)\zeta_2},$$

and

$$k_d^2=k^2-\frac{i4k}{d_3\zeta_2}. \tag{13}$$

3. Decoupling analysis

The analysis runs exactly as for the two-duct perforated element mufflers (Rao & Munjal 1984). The three second-order differential equations (10), (11) and (12) are first reduced to six first-order linear equations. Treating the differential operator as an algebraic variable, these six equations are decoupled through an eigenvalue analysis and the use of principal coordinates. Finally acoustic state variables at $z = 0$ are related to those at $z = l$ through a matrix, which is the required transfer matrix.

Denoting d/dz by prime ($'$), and defining

$$\dot{p}_1 = y_1,\ \dot{p}_2 = y_2,\ \dot{p}_3 = y_3,\ p_1 = y_4,$$
$$p_2 = y_5 \quad \text{and} \quad p_3 = y_6, \tag{14}$$

(10), (11) and (12) may be written in the form

$$\begin{bmatrix} -1 & 0 & 0 & D & 0 & 0 \\ 0 & -1 & 0 & 0 & D & 0 \\ 0 & 0 & -1 & 0 & 0 & D \\ D & 0 & 0 & \alpha_1 D+\alpha_2 & \alpha_3 D+\alpha_4 & 0 \\ 0 & D & 0 & \alpha_5 D+\alpha_6 & \alpha_7 D+\alpha_8 & \alpha_9 D+\alpha_{10} \\ 0 & 0 & D & 0 & \alpha_{11} D+\alpha_{12} & \alpha_{13} D+\alpha_{14} \end{bmatrix} \begin{bmatrix} y_1 \\ y_2 \\ y_3 \\ y_4 \\ y_5 \\ y_6 \end{bmatrix} = \begin{bmatrix} 0 \\ 0 \\ 0 \\ 0 \\ 0 \\ 0 \end{bmatrix} \tag{15a}$$

or

$$[\Delta]\{y\} = \{0\}, \tag{15b}$$

where

$$\alpha_1 = \frac{-iM_1}{1-M_1^2}\left(\frac{k_a^2+k^2}{k}\right),\ \alpha_2 = \frac{k_a^2}{1-M_1^2},\ \alpha_3 = \frac{iM_1}{1-M_1^2}\left(\frac{k_a^2-k^2}{k}\right),$$

$$\alpha_4 = \frac{k_a^2-k^2}{1-M_1^2},\quad \alpha_5 = \frac{iM_2}{1-M_2^2}\left(\frac{k_b^2-k^2}{k}\right),\quad \alpha_6 = -\frac{(k_b^2-k^2)}{1-M_2^2},$$

$$\alpha_7 = \frac{-iM_2}{1-M_2^2}\left(\frac{k_b^2+k_c^2}{k}\right),\ \alpha_8 = \frac{k_b^2+k_c^2-k^2}{1-M_2^2},\ \alpha_9 = \frac{iM_2}{1-M_2^2}\left(\frac{k_c^2-k^2}{k}\right),$$

$$\alpha_{10} = \frac{-(k_c^2-k^2)}{1-M_2^2},\ \alpha_{11} = \frac{iM_3}{1-M_3^2}\left(\frac{k_d^2-k^2}{k}\right),\ \alpha_{12} = -\frac{k_d^2-k^2}{1-M_3^2},$$

$$\alpha_{13} = \frac{-iM_3}{1-M_3^2}\left(\frac{k_d^2+k^2}{k}\right),\ \alpha_{14} = \frac{k_d^2}{1-M_3^2}, \tag{16}$$

and

$$D \equiv \frac{\mathrm{d}}{\mathrm{dz}}. \tag{17}$$

Making use of principal coordinates, these equations may be decoupled.

The new variables, i.e., the principal co-ordinates Γ_1, Γ_2, Γ_3, Γ_4, Γ_5 and Γ_6 are related to variables y_1, y_2, y_3, y_4, y_5 and y_6, through the modal matrix $[\Psi]$ as

$$\{y\} = [\Psi]\{\Gamma\} \tag{18}$$

where

$$\Psi_{1,j} = 1{\cdot}0 \quad \text{(say)},$$

$$\Psi_{2,j} = -(\beta_j^2 + \alpha_1\beta_j + \alpha_2)/(\alpha_3\beta_j + \alpha_4),$$

$$\Psi_{3,j} = \frac{(\beta_j^2 + \alpha_1\beta_j + \alpha_2)\,(\beta_j^2 + \alpha_7\beta_j + \alpha_8) - (\alpha_3\beta_j + \alpha_4)\,(\alpha_5\beta_j + \alpha_6)}{(\alpha_3\beta_j + \alpha_4)\,(\alpha_9\beta_j + \alpha_{10})},$$

$$\Psi_{4,j} = 1{\cdot}0/\beta_j\,,$$

$$\Psi_{5,j} = \Psi_{2,j}/\beta_j\,,$$

and

$$\Psi_{6,j} = \Psi_{3,j}/\beta_j\,, \tag{19}$$

and subscript j takes the values 1, 2 . . . , 6. β's are roots of the sixth degree polynomial

$$|\Delta| = 0, \tag{20}$$

to be found numerically on a computer by means of one of the standard subroutines.

The general solutions to first order equations (20) can be obtained as

$$\Gamma_j(z) = C_j e^{\beta_j z}, \tag{21}$$

where subscript j takes values 1, 2, . . . 6.

Next, (4), (5) and (6) may be used to obtain expressions for $w_1(z)$, $w_2(z)$ and $w_3(z)$. Finally, we may write

$$\begin{bmatrix} p_1(z) \\ p_2(z) \\ p_3(z) \\ \rho_0 c_0 w_1(z) \\ \rho_0 c_0 w_2(z) \\ \rho_0 c_0 w_3(z) \end{bmatrix} = [A] \begin{bmatrix} C_1 \\ C_2 \\ C_3 \\ C_4 \\ C_5 \\ C_6 \end{bmatrix}, \tag{22}$$

where elements $A_{i,j}$ involving only M, k and l are given by expressions noted in appendix A.

Now the pressure and velocity at $z = 0$ can be related to the pressure and velocity at $z = l$; that is,

$$\begin{bmatrix} p_1(0) \\ p_2(0) \\ p_3(0) \\ \rho_0 c_0 w_1(0) \\ \rho_0 c_0 w_2(0) \\ \rho_0 c_0 w_3(0) \end{bmatrix} = [T] \begin{bmatrix} p_1(l) \\ p_2(l) \\ p_3(l) \\ \rho_0 c_0 w_1(l) \\ \rho_0 c_0 w_2(l) \\ \rho_0 c_0 w_3(l) \end{bmatrix}, \tag{23}$$

where the transfer matrix is given by

$$[T] = [A(0)]\,[A(l)]^{-1}. \tag{24}$$

4. Transfer matrix for cross-flow expansion chamber

To eliminate four of the six state variables in the foregoing general solution, (23), we make use of four boundary conditions. In the case of cross-flow expansion chamber with rigid end termination, the boundary conditions are (Thawani & Jayaraman 1983)

$$\begin{aligned} z = 0 &: \rho_0 c_0 w_2(0) = -i \tan(k\, l_a)\, p_2(0) \\ z = 0 &: \rho_0 c_0 w_3(0) = -i \tan(k\, l_a)\, p_3(0) \\ z = l &: \rho_0 c_0 w_1(l) = -i \tan(k\, l_b)\, p_1(l) \\ z = l &: \rho_0 c_0 w_2(l) = -i \tan(k\, l_b)\, p_2(l). \end{aligned} \tag{25}$$

Skipping the elimination details, the final expressions for the upstream state variables and the downstream variables can be written as (Rao 1984)

$$\begin{bmatrix} p_1(0) \\ \rho_0 c_0 w_1(0) \end{bmatrix} = \begin{bmatrix} T_a & T_b \\ T_c & T_d \end{bmatrix} \begin{bmatrix} p_3(l) \\ \rho_0 c_0 w_3(l) \end{bmatrix} \tag{26}$$

The expressions for T are given in appendix B.

5. Transfer matrix for reverse flow expansion chamber

The following changes have to be noted in this element:
(a) mean flow in duct three is negative with respect to the reference direction;
(b) the boundary conditions are different; these are

$$\begin{aligned} z = 0 &: \rho_0 c_0 w_2(0) = -i \tan(k\, l_a)\, p_2(0) \\ z = l &: \rho_0 c_0 w_1(l) = -i \tan(k\, l_b)\, p_1(l) \\ z = l &: \rho_0 c_0 w_2(l) = -i \tan(k\, l_b)\, p_2(l) \\ z = l &: \rho_0 c_0 w_3(l) = -i \tan(k\, l_b)\, p_3(l). \end{aligned} \tag{27}$$

Skipping the algebraic details of the elimination process, the transfer matrix relation for this element may be written as (Rao 1984)

$$\begin{bmatrix} p_1(0) \\ \rho_0 c_0 w_1(0) \end{bmatrix} = \begin{bmatrix} T_a & T_b \\ T_c & T_d \end{bmatrix} \begin{bmatrix} p_3(0) \\ -\rho_0 c_0 w_3(0) \end{bmatrix}, \tag{28}$$

and the resulting expressions for T_a, T_b, T_c and T_d are given in appendix C (Rao 1984).

6. Experimental evidence

In order to test the validity of the mathematical model at various mean flow conditions, noise reduction measurements were made on typical three-duct perforated element muffler configurations of figure 1.

Noise reduction, NR, is the difference in sound pressure levels at two arbitrarily selected points in the exhaust pipe and the tail pipe, located upstream and downstream of the muffler proper, respectively. Referring to figure 1,

$$\text{NR} = SPL_1 - SPL_3 = 20 \log_{10} |p_1/p_3| \,, \tag{29}$$

where p denotes the root mean square value of the acoustic pressure perturbation.

For the purpose of calculation, since p_1 is not known directly, one can write

$$p_1/p_3 = (p_1/p_0)\cdot(p_0/p_3), \tag{30}$$

where p_0 is the acoustic pressure at the radiation end. Applying the wave relationships for the pipe section of length l_e, one obtains (Munjal 1986)

$$(p_3/p_0) = \cos k_0 l_e + (iY_3/Z_0) \sin k_0 l_e, \tag{31}$$

where Z_0 is the radiation impedance, p_0/v_0. (32)

The other pressure ratio p_1/p_0 may be obtained from the transfer matrix relation

$$\begin{bmatrix} p_1 \\ v_1 \end{bmatrix} = \begin{bmatrix} T_{11} & T_{12} \\ T_{21} & T_{22} \end{bmatrix} \begin{bmatrix} p_0 \\ v_0 \end{bmatrix}, \tag{33}$$

where v denotes acoustic mass velocity, $\rho_0 Au$, and T_{ij} $(i, j = 1, 2)$ are the four-pole parameters of the overall transfer matrix relating the state variables at points 1 and 0. This matrix is a product of the transfer matrices of the upstream pipe, perforated element, and downstream pipe.

From (32) and (33) we obtain

$$(p_1/p_0) = T_{11} + T_{12}/Z_0. \tag{34}$$

Equations (29), (30), (31) and (34) may be combined to obtain

$$\text{NR} = 20 \log_{10} \left| \frac{T_{11} + T_{12}/Z_0}{\cos k_0 l_e + iY_3/Z_0 \cdot \sin k_0 l_e} \right| . \tag{35}$$

7. Results and discussion

General Fortran programs have been developed for computation (on DEC 10 computer) of noise reduction for three-duct element configurations shown in figure 1 over the frequency range covered by pure plane wave propagation, in steps of 20 Hz. The following perforated impedances were incorporated in the noise reduction prediction (Sullivan 1979),

$$\zeta = (6\times10^{-3} + i4{\cdot}8\times10^{-5} f)/\sigma, \quad \text{for } M = 0,$$

$$\zeta = (0{\cdot}514\ \mathrm{d}M/l\sigma + i4{\cdot}8\times10^{-5} f)/\sigma, \quad \text{for } M \geq 0{\cdot}05.$$

Figure 2 shows the typical curves of noise reduction versus frequency of three-duct cross-flow muffler represented in figure 1a for a stationary medium ($M = 0$ condition). Neglecting the temperature gradient and the tube wall thickness, there is good agreement between the predictions of the present investigation and those of experimental results. In figures 3 and 4 a similar exercise is repeated for inlet flow, Mach number $M = 0{\cdot}10$ and $M = 0{\cdot}2$. Though there are small discrepancies, yet the agreement between theory and experiment is generally good.

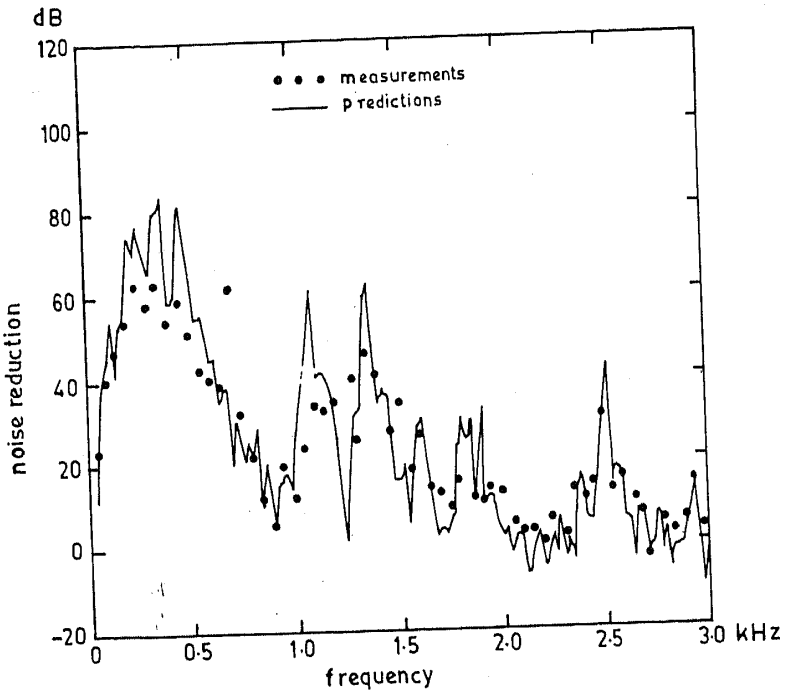

Figure 2. Noise reduction of three-duct cross-flow expansion chamber of figure 1a for $M_1 = 0$.

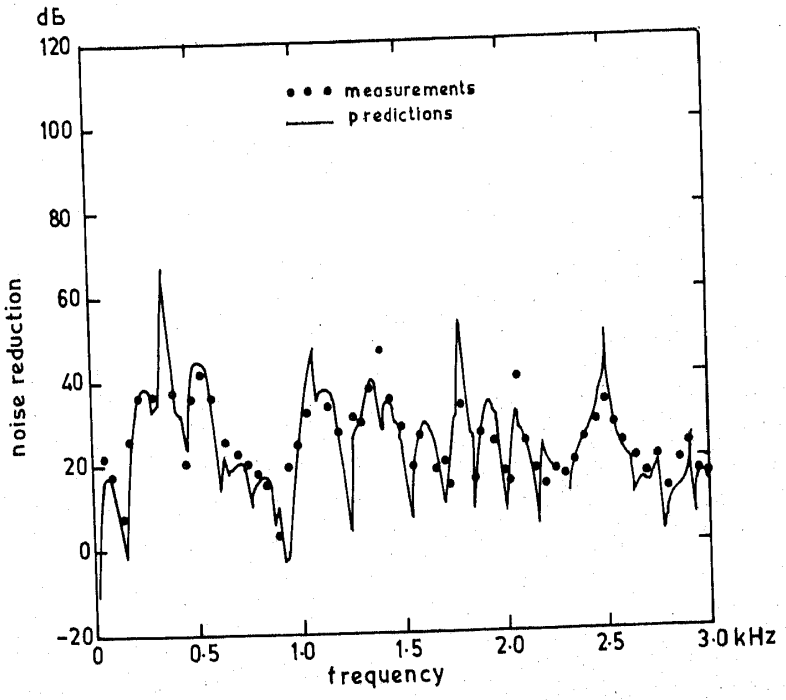

Figure 3. Noise reduction of three-duct cross-flow expansion chamber of figure 1a for $M_1 = 0{\cdot}1$.

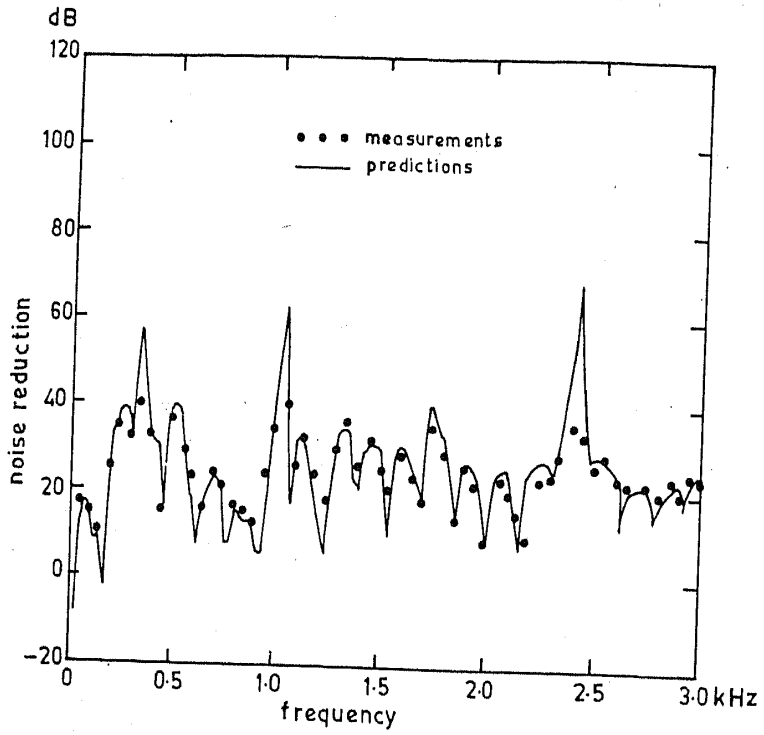

Figure 4. Noise reduction of three-duct cross-flow expansion chamber of figure 1a for $M_1 = 0{\cdot}2$.

Noise reduction at zero mean flow of the reverse-flow expansion chamber of figure 1b is shown in figure 5. The agreement between theoretical predictions and experimental observations is good in terms of peak locations as well as magnitudes. Figures 6 and 7 present computed and experimental noise reduction curves for the same muffler with $M = 0{\cdot}1$ and $M = 0{\cdot}2$ respectively. Here too, the theoretical results match the experimental results well.

In general, experimental values of noise reduction are in good agreement with the predicted results, thereby substantiating the validity of the transfer matrices derived and used in the predictions.

These transfer matrices may be used along with those for other non-perforated elements like a tube, sudden contraction, sudden expansion, extended inlet, extended outlet, flow-reversal contraction and flow-reversal expansion (Munjal 1975; Panicker & Munjal 1981), to predict the overall performance (in terms of insertion loss, transmission loss, level difference or noise reduction) of a given muffler. These performance curves for typical dimensions may be used for table-design of an efficient muffler, keeping in mind other non-acoustical considerations like overall size, weight, cost of fabrication, back pressure on the engine, durability etc. (Munjal 1986).

The first author would like to thank the authorities of the Osmania University for the study leave granted. The second author acknowledges with thanks the financial support received from the Stiftung Volkswagenwerk, Hannover, Germany, for a project in collaboration with Professor M Heckl and Professor M Hubert of the Technische Universität Berlin.

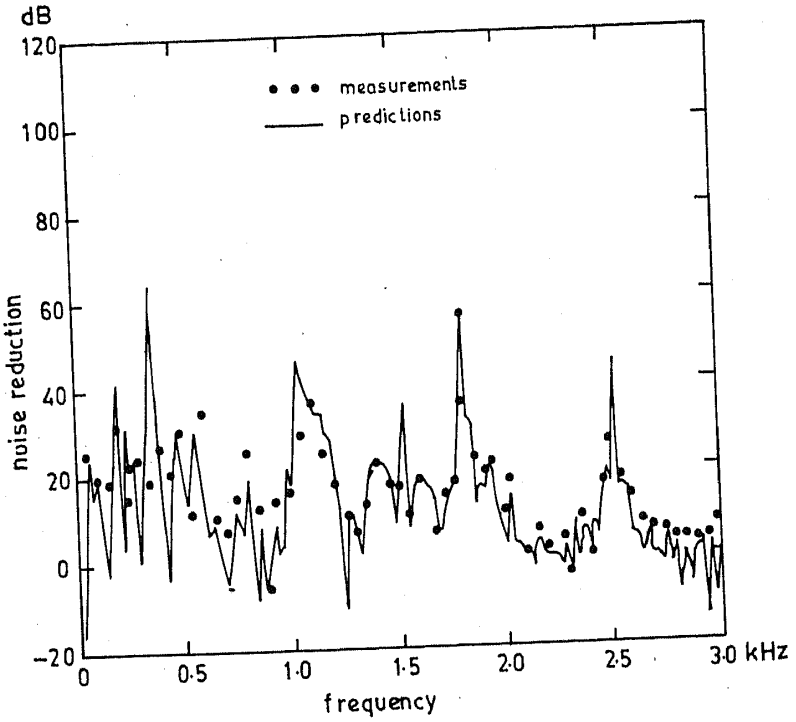

Figure 5. Noise reduction of three-duct reverse-flow expansion chamber of figure 1b for $M_1 = 0$.

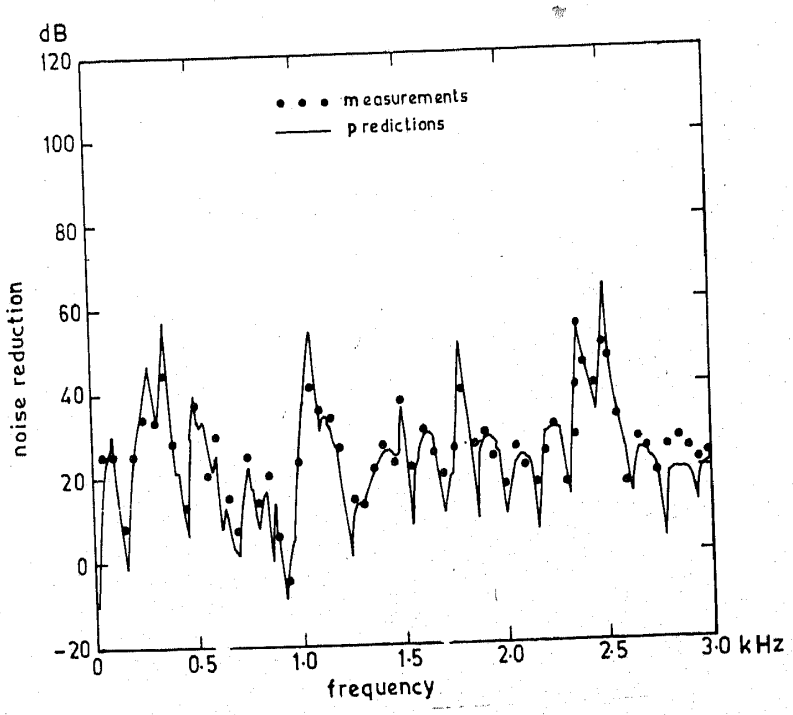

Figure 6. Noise reduction of three-duct reverse-flow expansion chamber of figure 1b for $M_1 = 0{\cdot}1$.

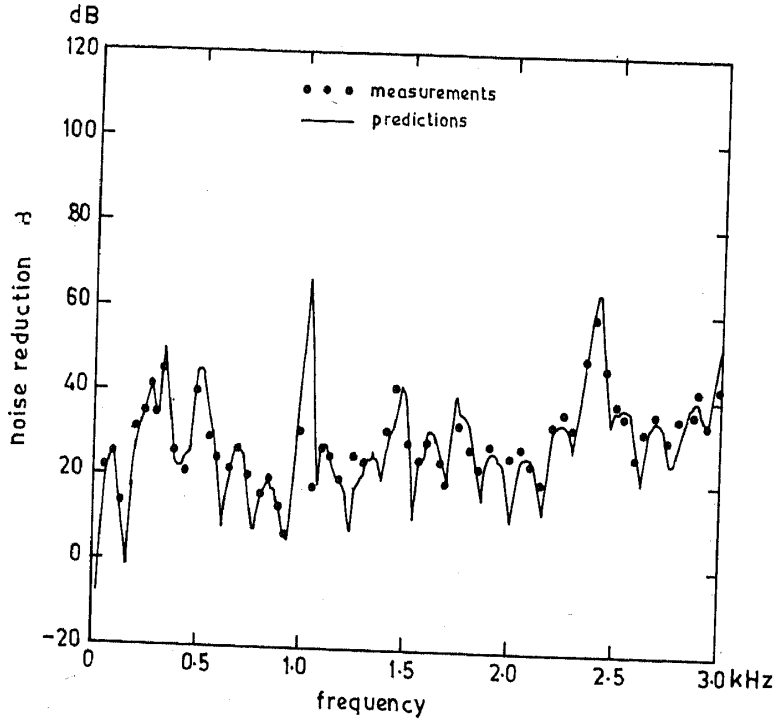

Figure 7. Noise reduction of three-duct reverse-flow expansion chamber of figure 1b for $M_1 = 0{\cdot}2$.

Appendix A

The following relations hold for both the three-duct cross-flow expansion chamber and the three-duct reverse flow expansion chamber.

$$A_{1,j} = \psi_{4,j} e^{\beta_j z},$$
$$A_{2,j} = \psi_{5,j} e^{\beta_j z},$$
$$A_{3,j} = \psi_{6,j} e^{\beta_j z},$$
$$A_{4,j} = -e^{\beta_j z}/(ik + M_1\beta_j),$$
$$A_{5,j} = -\psi_{2,j} e^{\beta_j z}/(ik + M_2\beta_j),$$
$$A_{6,j} = -\psi_{3,j} e^{\beta_j z}/(ik + M_3\beta_j).$$

Appendix B

The following relations hold for three-duct perforated element cross-flow expansion chamber:

$$T_a = TT_{1,2} + A_3C_3; \quad T_b = TT_{1,4} + B_3C_3;$$
$$T_c = TT_{3,2} + A_3D_3; \quad T_d = TT_{3,4} + B_3D_3;$$
$$A_3 = (TT_{2,2}X_2 - TT_{4,2})/F_2; \quad B_3 = (TT_{2,4}X_2 - TT_{4,4})/F_2;$$

$$C_3 = TT_{1,1} + X_1 TT_{1,3}; \quad D_3 = TT_{3,1} + X_1 TT_{3,3};$$
$$F_2 = TT_{4,1} + X_1 TT_{4,3} - X_2(TT_{2,1} + X_1 TT_{2,3}).$$

$[TT]$ is an intermediate 4×4 matrix defined as

$$\begin{bmatrix} p_1(0) \\ p_2(0) \\ \rho_0 c_0 w_1(0) \\ \rho_0 c_0 w_2(0) \end{bmatrix} = [TT]_{4\times4} \begin{bmatrix} p_2(l) \\ p_3(l) \\ \rho_0 c_0 w_2(l) \\ \rho_0 c_0 w_2(l) \end{bmatrix},$$

with

$$TT_{1,1} = A_1 A_2 + T_{1,2}; \quad TT_{1,2} = B_1 A_2 + T_{1,3};$$
$$TT_{1,3} = C_1 A_2 + T_{1,5}; \quad TT_{1,4} = D_1 A_2 + T_{1,6};$$
$$TT_{2,1} = A_1 B_2 + T_{2,2}; \quad TT_{2,2} = B_1 B_2 + T_{2,3};$$
$$TT_{2,3} = C_1 B_2 + T_{2,5}; \quad TT_{2,4} = D_1 B_2 + T_{2,6};$$
$$TT_{3,1} = A_1 C_2 + T_{4,2}; \quad TT_{3,2} = B_1 C_2 + T_{4,3};$$
$$TT_{3,3} = C_1 C_2 + T_{4,5}; \quad TT_{3,4} = D_1 C_2 + T_{4,6};$$
$$TT_{4,1} = A_1 D_2 + T_{5,2}; \quad TT_{4,2} = B_1 D_2 + T_{5,3};$$
$$TT_{4,3} = C_1 D_2 + T_{5,5}; \quad TT_{4,4} = D_1 D_2 + T_{5,6};$$
$$A_1 = (T_{3,2} X_2 - T_{6,2})/F_1; \quad B_1 = (T_{3,3} X_2 - T_{6,3})/F_1;$$
$$C_1 = (T_{3,5} X_2 - T_{6,5})/F_1; \quad D_1 = (T_{3,6} X_2 - T_{6,6})/F_1;$$
$$A_2 = T_{1,1} + X_1 T_{1,4}; \quad B_2 = T_{2,1} + X_1 T_{2,4};$$
$$C_2 = T_{4,1} + X_1 T_{4,4}; \quad D_2 = T_{5,1} + X_1 T_{5,4};$$
$$F_1 = T_{6,1} + X_1 T_{6,4} - X_2(T_{3,1} + X_1 T_{3,4});$$
$$X_1 = i \tan(kl_b);$$

and

$$X_2 = -i \tan(kl_a).$$

Appendix C

The following relations hold only for three-duct perforated element reverse-flow expansion chamber

$$T_a = B_{1,1} D_{1,1} + B_{1,2} D_{2,1} + B_{1,3} D_{3,1},$$
$$T_b = B_{1,1} D_{1,2} + B_{1,2} D_{2,2} + B_{1,3} D_{3,2},$$
$$T_c = B_{4,1} D_{1,1} + B_{4,2} D_{2,1} + B_{4,3} D_{3,1},$$
$$T_d = B_{4,1} D_{1,2} + B_{4,2} D_{2,2} + B_{4,3} D_{3,2},$$

$$B_{i1,i2} = T_{i1,i2} + X_1 T_{i1,(i2+3)},$$

$$i1 = 1, 2, \ldots, 6,$$

$$i2 = 1, 2, 3,$$

$$X_1 = i \tan(kl_b).$$

$$D_{1,1} = C_{1,1} D_{2,1} + C_{1,3} D_{3,1},$$

$$D_{1,2} = C_{1,1} D_{2,2} + C_{1,2} D_{3,2},$$

$$D_{2,1} = C_{3,2}/F_4; \quad D_{2,2} = -C_{2,2}/F_4,$$

$$D_{3,1} = -C_{3,1}/F_4; \quad D_{3,2} = C_{2,1}/F_4,$$

$$F_4 = C_{2,1} C_{3,2} - C_{2,2} C_{3,1},$$

$$C_{1,1} = (B_{5,2} - X_2 B_{2,2})/F_3; \quad C_{1,2} = (B_{5,3} - X_2 B_{2,3})/F_3,$$

$$C_{2,1} = B_{3,2} + C_{1,1} B_{3,1}; \quad C_{2,2} = B_{3,3} + C_{1,2} B_{3,1},$$

$$C_{3,1} = B_{6,2} + C_{1,1} B_{6,1}; \quad C_{3,2} = B_{6,3} + C_{1,2} B_{6,1},$$

$$F_3 = B_{2,1} X_2 - B_{5,1},$$

$$X_2 = -i \tan(kl_a).$$

Appendix D. Notation

A_1, A_0	internal areas of inlet and exit pipes, respectively,
c_0	velocity of wave propagation
d	internal diameter of pipe
f	frequency,
i	iota, $\sqrt{-1}$,
k	wave number, (ω/c_0),
l	length of pipe,
M	Mach number, (W_0/c_0),
M_i	inlet Mach number,
M_0	exit Mach number,
p_0	pressure of the undisturbed fluid,
p	fluctuating pressure,
t	time co-ordinate,
temp	temperature,
$u_{1,2}, u_{2,3}$	radial fluctuating velocities at 1, 2 and 2, 3 interfaces of the control volume, respectively,
W_0	velocity of the undisturbed fluid,
w	fluctuating velocity,
Y	characteristic impedance, c_0/A,
z	axial co-ordinate,
ρ_0	density of undisturbed fluid,
ρ	fluctuation in density,
ω	circular frequency,
ζ_1, ζ_2	acoustical impedances at 1, 2 and 2, 3 interfaces, respectively.

References

Munjal M L 1975 *J. Sound Vib.* 39: 105–119
Munjal M L 1986 *Acoustics of ducts and mufflers* (New York: John Wiley) (in print)
Panicker V B, Munjal M L 1981a *J. Indian Inst. Sci.* A63: 1–19
Panicker V B, Munjal M L 1981b *J. Indian Inst. Sci.* A63: 21–38
Rao K N 1984 *Prediction and verification of the aero-acoustic performance of perforated element mufflers*, Ph.D. thesis, Indian Institute of Science, Bangalore
Rao K N, Munjal M L 1984 A generalized decoupling method for analysing perforated element mufflers, Proceedings of the Nelson Acoustics Conference, Madison, USA
Sullivan J W 1979a *J. Acoust. Soc. Am.* 66: 772–778
Sullivan J W 1979b *J. Acoust. Soc. Am.* 66: 779–788
Sullivan J W, Crocker M J 1978 *J. Acoust. Soc. Am.* 64: 207–215
Thawani P T, Jayaraman K 1983 *J. Acoust. Soc. Am.* 73: 1387–1389